Elsevier Editorial System(tm) for
Neurobiology of Disease

Manuscript Draft

Manuscript Number:

Title: Altered mechanisms underlying the abnormal glutamate release in amyotrophic lateral sclerosis at a pre-symptomatic stage of the disease

Article Type: Research paper

Keywords: amyotrophic lateral sclerosis; pre-symptomatic SOD1G93A mice; excessive glutamate release; glutamate excitotoxicity; glutamate release mechanisms; presynaptic proteins; Synapsin-I; glycogen synthase kinase 3.

Corresponding Author: Prof. Giambattista Bonanno, Chemistry and Pharmaceutical Technology

Corresponding Author's Institution: University of Genoa

First Author: Tiziana Bonifacino, Chemistry and Pharmaceutical Technology

Order of Authors: Tiziana Bonifacino, Chemistry and Pharmaceutical Technology; Laura Musazzi; Marco Milanese, Chemistry and Pharmaceutical Technology ; Mara Seguini; Antonella Marte, Chemistry and Pharmaceutical Technology ; Elena Gallia, Pharmacy; Luca Cattaneo, Chemistry and Pharmaceutical Technology ; Franco Onofri; Maurizio Popoli; Giambattista Bonanno, Chemistry and Pharmaceutical Technology

Abstract: Abnormal Glu release occurs in the spinal cord of SOD1G93A mice, a transgenic animal model for human ALS. Here we studied the mechanisms underlying Glu release in spinal cord nerve terminals of SOD1G93A mice at a pre-symptomatic disease stage (30 days) and found that the basal release of Glu was more elevated in SOD1G93A respect to SOD1 mice, and that the surplus of release rely on synaptic vesicle exocytosis. Exposure to high KCl or ionomycin provoked Ca2+-dependent Glu release that was likewise augmented in SOD1G93A mice. Equally, the Ca2+-independent hypertonic sucrose-induced Glu release was abnormally elevated in SOD1G93A mice. Also in this case, the surplus of Glu release was exocytotic in nature. We could determine elevated cytosolic Ca2+ levels, increased phosphorylation of Synapsin-I, which was causally related to the abnormal Glu release measured in spinal cord synaptosomes of pre-symptomatic SOD1G93A mice, and increased phosphorylation of glycogen synthase kinase-3 at the inhibitory sites, an event that favours SNARE protein assembly. Western blot experiments revealed an increased number of SNARE protein complexes at the nerve terminal membrane, with no changes of the three SNARE proteins and increased expression of Synaptotagmin-1 and β-Actin but not of an array of other release-related presynaptic proteins. These results indicate that the abnormal exocytotic Glu release in spinal cord of pre-symptomatic SOD1G93A mice is mainly based on the increased size of the readily releasable pool of vesicles and release facilitation, supported by plastic changes of specific presynaptic mechanisms.

Suggested Reviewers: Pamela J Shaw
pamela.shaw@sheffield.ac.uk

*Manuscript
Click here to view linked References

Altered mechanisms underlying the abnormal glutamate release in amyotrophic lateral sclerosis at a pre-symptomatic stage of the disease

Tiziana Bonifacino [a,*], Laura Musazzi [b,*], Marco Milanese [a], Mara Seguini [b], Antonella Marte [c], Elena Gallia [a], Luca Cattaneo [a], Franco Onofri [c], Maurizio Popoli [b,*], Giambattista Bonanno [a,*]

* Equally contributed

[a] Department of Pharmacy, Unit of Pharmacology and Toxicology, and Center of Excellence for Biomedical Research, University of Genoa, 16148 Genoa, Italy; [b] Department of Pharmacological and Biomolecular Sciences and Center of Excellence on Neurodegenerative Diseases, University of Milan, 20133 Milan, Italy; [c] Department of Experimental Medicine, Unit of Human Physiology, University of Genoa, Viale Benedetto XV, 16132 Genoa, Italy.

e-mail addresses: bonifacino@difar.unige.it; laura.musazzi@unimi.it; milanese@difar.unige.it; mara.seguini@unimi.it; antonella.marte@unige.it; gallia@difar.unige.it; cattaneo@difar.unige.it; franco.onofri@unige.it; maurizio.popoli@unimi.it; bonanno@difar.unige.it.

Corresponding author:

Prof. Giambattista Bonanno, University of Genoa, Department of Pharmacy, Viale Cembrano 4, 16148 Genoa, Italy. Tel: +39 010 3532658. bonanno@difar.unige.it

Abstract

Abnormal Glu release occurs in the spinal cord of SOD1^{G93A} mice, a transgenic animal model for human ALS. Here we studied the mechanisms underlying Glu release in spinal cord nerve terminals of SOD1^{G93A} mice at a pre-symptomatic disease stage (30 days) and found that the basal release of Glu was more elevated in SOD1^{G93A} respect to SOD1 mice, and that the surplus of release rely on synaptic vesicle exocytosis. Exposure to high KCl or ionomycin provoked Ca^{2+}-dependent Glu release that was likewise augmented in SOD1^{G93A} mice. Equally, the Ca^{2+}-independent hypertonic sucrose-induced Glu release was abnormally elevated in SOD1^{G93A} mice. Also in this case, the surplus of Glu release was exocytotic in nature. We could determine elevated cytosolic Ca^{2+} levels, increased phosphorylation of Synapsin-I, which was causally related to the abnormal Glu release measured in spinal cord synaptosomes of pre-symptomatic SOD1^{G93A} mice, and increased phosphorylation of glycogen synthase kinase-3 at the inhibitory sites, an event that favours SNARE protein assembly. Western blot experiments revealed an increased number of SNARE protein complexes at the nerve terminal membrane, with no changes of the three SNARE proteins and increased expression of Synaptotagmin-1 and β-Actin but not of an array of other release-related presynaptic proteins. These results indicate that the abnormal exocytotic Glu release in spinal cord of pre-symptomatic SOD1^{G93A} mice is mainly based on the increased size of the readily releasable pool of vesicles and release facilitation, supported by plastic changes of specific presynaptic mechanisms.

Key words: amyotrophic lateral sclerosis; pre-symptomatic SOD1^{G93A} mice; excessive glutamate release; glutamate excitotoxicity; glutamate release mechanisms; presynaptic proteins; Synapsin-I; glycogen synthase kinase 3.

Abbreviations: α/β-SNAP, α/β solube NSF attachment proteins; ALS, amyotrophic lateral sclerosis; BoNt-C1, Botulinum Neurotoxin C1; β-Tub III, β-Tubulin III; $[Ca^{2+}]_c$, cytosolic calcium concentration; CaMK-II, Ca2+/calmodulin-dependent protein kinase II; DL-TBOA, DL-threo-beta-benzyloxyaspartate; GSK-3, glycogen synthase kinase 3; HEPES, 4-(2-hydroxyethyl)-1-piperazineethanesulfonic acid; [^{3}H]D-Asp, [^{3}H]D-Aspartate; mAbs, monoclonal antibodies; MNs, motor neurons; Munc-13, mammalian uncoordinated-13; Munc-18, mammalian uncoordinated-18; NSF, N-ethylamide sensitive fusion protein; Rab-3A, Ras-related protein 3A; RRP, readily releasable pool; SNAP-25, Synaptosome-associated protein of 25kDa; SOD1, superoxide dismutase-1; SNARE, soluble NSF attachment protein receptors; Stx-1, Syntaxin 1; Syn-I, synapsin-I; Syph-1, Synaptophysin 1; Syt-1, synaptotagmin 1; VAMP-2, Vesicular associate membrane protein 2.

Introduction

Amyotrophic lateral sclerosis (ALS) is a fatal neuromuscular disorder characterized by degeneration of cortical, brainstem and spinal motor neurons (MNs) leading to muscle wasting, weakness and spasticity (Brown et al, 1995; Eisen, 2009). Although the clinical outcome in ALS is defined by MN degeneration, the disease is non-cell autonomous, also involving astrocytes, microglia and oligodendrocytes (Boillèe et al., 2006; Haidet-Phillips et al., 2011; Ilieva et al., 2009;).

ALS has an incidence of 2–3 new cases/year per 100,000 individuals and it is most commonly sporadic, although familial forms represent about 10% of patients (Andersen and Al-Chalabi, 2011). The first identified ALS-linked gene was superoxide dismutase-1 (SOD1) that accounts for about 20% of patients with familial ALS (Birve et al., 2010; Mulder et al., 1986; Rosen et al., 1993). So far, at least fifteen more genes involved in different cellular pathways have been associated to ALS (Andersen and Al-Chalabi, 2011), thus indicating that multiple cellular events contribute to the disease. They include oxidative stress, mitochondrial dysfunction, protein aggregation, impaired axonal transport, neuroinflammation, dysregulated RNA signaling, immunological imbalance and glutamate(Glu)-mediated excitotoxicity (Cleveland et al., 1996; King et al., 2016; Morrison and Morrison, 1999; Peters et al., 2015; Tan et al., 2014; Van Den Bosch et al., 2006).

Strong evidence support the notion that altered excitatory transmission in spinal cord and excitotoxicity, based on high levels of extra-cellular Glu and abnormal function of postsynaptic Glu receptors at lower MNs, plays a major role in disease progression and cell death (Kuner et al., 2005; Shaw and Eggett, 2000; Tortarolo et al., 2006; Van Damme et al., 2005; Van Den Bosch et al., 2000; Wuolikainen et al., 2011). Elevation of Glu concentration in plasma and cerebrospinal fluid has been documented in ALS patients (Perry et al., 1990; Rothstein et al., 1990; Shaw et al., 1995; Spreux-Varoquaux et al., 2002; Wuolikainen et al., 2011) and impaired clearance of Glu by

astrocyte uptake, due to reduced expression of Glu transporter 1, has been proposed as a cause of neurotoxicity (Cleveland and Rothstein, 2001; Rothstein et al., 1995), although the hypothesis that Glu transport dysfunction is a primary event for MN death in spinal cord has been disputed (Corona and Tapia, 2004; Tovar-Y-Romo et al., 2009).

More recent studies of our group with mice expressing human SOD1 carrying the G93A point mutation ($SOD1^{G93A}$) indicated that neuronal Glu release, under basal condition and upon exposure to different releasing stimuli, including nerve terminal depolarization, is abnormally high in the spinal cord of these animals at the late stage of disease. We found that increased cytosolic calcium concentration ($[Ca^{2+}]_c$), the associated over-activation of Ca^{2+}/calmodulin-dependent protein kinase II (CaMK-II), which has been already shown in sporadic ALS patients (Hu et al., 2003) and, in turn, the phosphorylation of Synapsin I (Syn-I), an event that contributes to fill up the readily releasable pool (RRP) of vesicles and to boost vesicles fusion, supports the stimulus-evoked Glu release (Milanese et al., 2011). The higher exocytotic release of Glu is detectable also at the early-symptomatic and pre-symptomatic stages of the disease. This precociousness fosters the hypothesis that the increased release of Glu represents a pivotal factor in the pathology rather than a consequence of disease progression, pointing to this mechanism in the panorama of the ALS causes.

Whereas the mechanisms supporting excessive Glu release at the late stage of the disease have been, at least in part, elucidated no studies are available at pre-symptomatic stages. In this work, we report that the abnormal Glu release in 30 day-old pre-symptomatic $SOD1^{G93A}$ mice is exocytotic and that augmentation of $[Ca^{2+}]_c$ and of the number of soluble NSF attachment protein receptors (SNARE) complexes seem to be major causes for the augmented neurotransmitter release. Moreover, we found selective molecular changes in spinal cord nerve terminals, including increased phosphorylation/activation of Syn-I, increased expression of Synaptotagmin 1 (Syt-1) and β-Actin, inhibition of glycogen synthase kinase 3 (GSK-3), all of which may be related to the abnormal Glu release.

Materials and methods

Animals

B6SJL-TgN SOD1/G93A(+)1Gur mice expressing high copy number of mutant human SOD1 with a $Gly^{93}Ala$ substitution [$SOD1^{G93A}$] and B6SJL-TgN (SOD1)2Gur mice expressing wild-type human SOD1 (SOD1) (Gurney et al., 1994) were originally obtained from Jackson Laboratories (Bar Harbor, ME) and bred at the animal facility of the Pharmacology and Toxicology Unit, Department of Pharmacy in Genoa. Transgenic animals have been crossed with background-matched B6SJL wild type female and selective breeding maintained each transgene in the hemizygous state. All transgenic mice were identified analyzing extracts from tail tips (homogenized in phosphate-buffer saline, freeze/thawed twice and centrifuged at 23,000 x *g* for 15 min at 4° C) by staining for SOD1 after polyacrylamide gel electrophoresis (10 % resolving and 4 % stacking) (Laemmli et al., 1970, Stifanese et al., 2010). Animals were housed at constant temperature (22 ± 1° C) and relative humidity (50%) under a regular dark-light schedule (light on 7 a.m. to 7 p.m.). Food and water were freely available. Animals of either sex were randomly divided into different experimental groups. All experiments were carried out in accordance with the guidelines established by the European Communities Council (EU Directive 114 2010/63/EU for animal experiments published on September 22nd, 2010) and with the Italian D.L. n. 26/2014, and were approved by the Italian Ministry of Health (Prot. No. 31754-3). All efforts were made to minimize animal suffering and to use only the number of animals necessary to produce reliable results. All the performed experiments using animals comply with the ARRIVE guidelines.

Preparation of synaptosomes

Animals were euthanized and the whole spinal cord rapidly removed. Synaptosomes were prepared essentially as described previously (Raiteri et al., 2008). The tissue was homogenized in

14 volumes of 0.32 M sucrose, buffered at pH 7.4 with Tris-HCl, using a glass-teflon tissue grinder (clearance 0.25 mm). The homogenate was centrifuged (5 min, 1,000 x *g* at 4° C) to remove nuclei and debris and the supernatant was gently stratified on a discontinuous Percoll® (Sigma-Aldrich, St Louis, Missouri, USA) gradient (2, 6, 10 and 20% v/v in Tris-buffered sucrose). After centrifugation at 33,500 x *g* for 5 min, the layer between 10 and 20% Percoll® (synaptosomal fraction) was collected, washed and resuspended in physiological medium having the following compositions (mM): NaCl, 140; KCl, 3; $MgSO_4$, 1.2; NaH_2PO_4, 1.2; $NaHCO_3$, 5; $CaCl_2$, 1.2; 4-(2-hydroxyethyl)-1-piperazineethanesulfonic acid (HEPES), 10; glucose, 10; pH 7.4 for $[Ca^{2+}]_c$ determination and release experiments or in lysis buffer for western blotting. Protein was measured according to Bradford (1976) using bovine serum albumin (Sigma-Aldrich, St Louis, Missouri, USA) as a standard. All the reagents were of laboratory grade.

Ca^{2+} determination

$[Ca^{2+}]_c$ was determined in spinal cord synaptosomes using the fluorescent dye fura-2/AM (Grynkiewicz et al., 1985). Synaptosomes were incubated for 40 min at 37° C, while gently shaking, in the HEPES-containing physiological medium, in the presence of 20 µM of $CaCl_2$ and 5 µM fura-2/AM (and 0.5% dimethyl sulfoxide (DMSO); Sigma-Aldrich, St Louis, Missouri, USA). Synaptosomes, incubated in the presence of 0.5% dimethyl sulfoxide only, were used to measure auto-fluorescence. After extra-synaptosomal fura-2/AM removal, the pellets were re-suspended in ice-cold standard or Ca^{2+}-free HEPES-buffered medium, divided into 200 µl aliquots (200 µg protein/sample), and stored on ice until use. Measures were obtained within 2 hours. Synaptosomes were diluted in HEPES-buffered medium containing the appropriate Ca^{2+} concentration (final volume 2 ml) and equilibrated at 37° C for 15 min. The measurements were made at 37° C under continuous stirring using an RF-5301PC dual wavelength spectrofluorophotometer (Shimadzu

Corporation, Milan, Italy) by alternating the excitation wavelengths of 340 and 380 nm. Fluorescent emission was monitored at 510 nm. Basal fluorescence was recorded for 1 min, then synaptosomes were exposed to KCl for additional 2 min. Calibration of the fluorescent signals was performed at the end of each measure by adding 10 μM ionomycin in the presence of $CaCl_2$ to obtain F_{max}, followed by 10 mM ethylene glycol tetraacetic acid; adjusted to pH 8.0 with 3 mM; Tris) to obtain F_{min}. After correcting for extracellular dye, $[Ca^{2+}]_c$ was calculated by the equation of Grynkiewicz et al. (1985), using a K_D of 224 nM for the Ca^{2+}-fura-2 complex. All the reagents were of laboratory grade.

Release experiments

Synaptosomes were incubated at 37° C for 15 min in the presence of 0.05 μM [^{3}H]D-Aspartate ([^{3}H]D-Asp, specific activity: 11.3 Ci/mmol was purchased from, Perkin Elmer Italia, Milan, Italy) a non-metabolizable analogue of Glu used to label the synaptosomal Glu releasing pools (Fleck et al., 2001; Wang et al., 2007; Raiteri et al., 2007). In a set of experiments synaptosomes were incubated 60 min in presence or in absence of 20 nM of Botulinum Neurotoxin C1 (BoNt-C1); in the last 15 min of incubation the radioactive label was introduced. In another set of experiments, synaptosomes were entrapped with antibodies that recognize the sites of phosphorylation of Syn-I, independently from their phospho/de-phospho state, during their preparation (Raiteri et al, 2000). Aliquots of the synaptosomal suspension were distributed on microporous filters placed at the bottom of a set of parallel superfusion chambers maintained at 37° C (Superfusion System; Ugo Basile, Comerio, IT; Raiteri et al., 1984). Superfusion was then started with standard medium at a rate of 0.5 ml/min and continued for 48 min. After 36 min of superfusion to equilibrate the system, samples were collected as follows: two 3-min samples (t =36-39 and 45-48 min; basal release) before and after one 6-min sample (t = 39-45 min; stimulus-evoked release). Stimulation with a 90 s pulse of 15 or 25 mM KCl or 0.3 or 1 μM ionomycin (Sigma-Aldrich, St

Louis, Missouri, USA) was applied at t = 39 min. In a set of experiments synaptosomes were exposed to a 15 s pulse of 150 mM sucrose at t = 39 min. In another set of experiments two consecutive 90 s depolarization pulses with 15 or 25 mM KCl were applied at t = 39 and 48 min of superfusion. When used, the Ca^{2+}-free medium was introduced at t = 20 min. The broad spectrum Glu uptake inhibitor *DL*-threo-beta-benzyloxyaspartate (DL-TBOA) (Tocris Bioscience, Bristol, UK; Shimamoto et al., 1998) was introduced at t = 30 min.

Radioactivity was determined in each sample collected and in the superfused filters by liquid scintillation (Ultima Gold, Perkin Elmer, Milan, Italy) counting. Tritium released in each sample was calculated as fractional rate x 100 (percentage of the total synaptosomal neurotransmitter content at the beginning of the respective sample collection). The stimulus-evoked neurotransmitter overflow was estimated by subtracting the transmitter content of the two 3-min fractions representing the basal release from that in the 6-min fraction collected during and after the stimulating pulse. All the reagents were of laboratory grade.

Isolation of presynaptic membranes and presynaptic protein determination

Mouse spinal cord synaptosomes, obtained from $SOD1^{G93A}$ and SOD1, were lysed on ice in lysis buffer (120 mM NaCl, 20 mM HEPES pH 7.4, 0.1 mM EGTA, 0.1 mM 1,4-dithiothreitol (DTT), containing 20 mM NaF, 5 mM Na_2PO_4, 1 mM Na_2VO_4, and 2 mg/ml of protease inhibitor cocktail; Sigma-Aldrich, Milano, IT) and centrifuged at 28,500 × g for 30 min (Treccani et al., 2014). Synaptic membranes were suspended in phosphate-buffered saline and used for western blotting experiments by incubating polyvinylidene difluoride membranes containing electrophoresed proteins with monoclonal antibodies (mAbs) at appropriate dilutions, as previously described (Bonanno et al., 2005). β-Actin, β-Tubulin III (β-Tub III), Complexin 1/2, Dynamin I, GSK-3α, GSK-3β, mammalian uncoordinated-13 (Munc-13), mammalian uncoordinated-18 (Munc-18), Myosin Va, N-ethylamide sensitive fusion protein (NSF), α/β NSF attachment proteins (α/β-

SNAP), phospho-Ser^{21} GSK-3α, phospho-Ser^{9} GSK-3β, phospho-Tyr^{279} GSK-3α, phospho-Tyr^{216} GSK-3β, phospho-Ser^{9} (site 1) Syn-I, phospho-Ser$^{566/603}$ (site 3) Syn-I and phospho-Ser$^{62/67}$ (site 4/5) Syn-I, Ras-related protein 3A (Rab-3A), Syntaxin 1 (Stx-1), Syn-I, Synaptosome-associated protein of 25kDa (SNAP-25), vesicle associated membrane protein 2 (VAMP-2), Synaptophysin 1 (Syph-1), Syt-1, were analysed. MAbs were used as follows: VAMP-2 1:2000, SNAP-25 1:2000, Syph-1 1:2000, Munc-13 1:1000, Rab-3A 1:5000, Syt-1 1:3000 and Syn-I 1:2000 from Synaptic System (Goettingen, Germany); Stx-1 1:5000, α/β-SNAP 1:1000, β-Actin 1:10000, Myosin Va 1:1000, phospho-Tyr^{279} GSK-3α 1:1000 and phospho-Tyr^{316} GSK-3β 1:1000 from Sigma-Aldrich (St Louis, Missouri, USA); Munc-18 1:1000 from BD Bioscience (Milan, Italy); GSK-3α 1:500 and GSK-3β 1:500 from Merk Millipore (Milan, Italy); β-Tub III 1:5000 from Promega Italia (Milan, Italy). Polyclonal antibodies were used as follows: Complexin-1/2 1:1000 and Syn-I 1:2000 from Synaptic System (Goettingen, Germany); NSF 1:1000, phospho-Ser^{9} (site 1) Syn-I 1:1000 and phospho-Ser^{21} GSK-3α 1:500 from Cell Signaling Technology Europe (Leiden, The Netherlands); Dynamin-I 1:1000 from Fisher Scientific Italia (Milan, Italy); phospho-Ser^{9} GSK-3β 1:500, phospho-Ser$^{62/67}$ (site 4/5) Syn-I 1:500 from Merk Millipore (Milan, Italy); phospho-Ser$^{566/603}$ (site 3) Syn-I 1:1000 was kindly provided by drs. P. Greengard; The Rockefeller University, NY. After incubation with peroxidase-coupled secondary antibodies (anti-mouse 1:2000-1:10000 and anti rabbit 1:1000-1:3000 from Sigma-Aldrich, St Louis, Missouri, USA) protein bands were detected by using ECL^{TM} (GE Healthcare Life Sciences, Milan, Italy) or Super Signal Dura West (Fisher Scientific Italia, Milan, Italy). Standard curves were obtained by loading increasing amounts of samples on gels. All of the protein bands used were within linear range of standard curves, and normalized for β-Tub III level in the same membrane. Phospho-proteins were normalized for the respective total protein. Quantity One software (Bio-Rad Laboratories, Milan, Italy) was used for standardization and quantitation, as previously reported (Bonanno et al., 2005, Musazzi et al., 2014).

Measurement of SNARE complex

For detection of sodium dodecyl sulfate resistant SNARE complexes, western blotting was performed on purified synaptosomal membranes non-boiled before gel loading (Musazzi et al., 2010), incubating polyvinylidene difluoride membranes containing blotted proteins with mAbs for Stx-1 1:5000 (Sigma-Aldrich, St Louis, Missouri, USA) or VAMP-2 1:2000 (Synaptic System, Goettingen, Germany). The membranes were incubated with anti-mouse secondary antibody 1:4000 (Sigma-Aldrich, St Louis, Missouri, USA), and immunoreactive bands revealed with ECL^{TM} (GE Healthcare Life Sciences, Milan, Italy). Signal detection and quantitation were performed as for western blotting experiments. All bands were normalized for Stx-1 or VAMP-2 monomer levels in the same membrane. All reagents were of laboratory grade.

Statistics

Data are expressed as mean ± SEM and $p<0.05$ was considered significant. Statistical comparison of two means were performed by unpaired two-tailed Student's t-test while multiple comparisons were performed using the analysis of variance (two-way ANOVA) followed by the Bonferroni's post hoc test. Analyses were performed by means of Sigma Stat software (Systat Software, Inc., San Jose, CA, USA).

Results

Glu release was previously found abnormally increased in >120 day old, late symptomatic, SOD1^{G93A} mice (Milanese et al., 2011). The release of the excitatory neurotransmitter was augmented also at early stages of the pathology. In the present study we characterized the phenomenon in 30 day-old pre-symptomatic SOD1^{G93A} mice, compared to age-matched SOD1 control mice.

The release of [^{3}H]D-Asp from spinal cord synaptosomes is increased in pre-symptomatic SOD1^{G93A} mice.

Prior to experiments of release, $[Ca^{2+}]_c$ was measured in spinal cord synaptosomes of pre-symptomatic SOD1 and SOD1^{G93A} mice by means of the fluorescent dye Fura2/AM. Figure 1A shows that the basal $[Ca^{2+}]_c$ was significantly higher (about 80%; $p<0.001$, $F_{(1,31)}= 32.944$). in SOD1^{G93A} mice. Exposure to 25 mM KCl produced a further increase of $[Ca^{2+}]_c$ in both SOD1 and SOD1^{G93A} mice, which was significantly more elevated (about 50%; $p<0.001$, $F_{(1,31)}= 32.944$) in the latter animals.

Release experiments with spinal cord synaptosomes in superfusion showed that the basal outflow of [^{3}H]D-Asp was more pronounced (about 45%; $p=0.033$, $F_{(1,61)}=16.964$) in SOD1^{G93A} than in SOD1 mice (Figure 1B). Figure 1B also shows that the spontaneous release was not modified by omission of Ca^{2+} from the superfusion medium in both mouse strains, while it was significantly diminished (about 50% and 35% decrease vs. SOD1 and SOD1^{G93A} mice, respectively; $p=0.049$ and $p=0.038$, $F(1,61)=8.132$) by 10 μM DL-threo-beta-Benzyloxyaspartate (DL-TBOA), a blocker of the Glu transporters (Shimamoto et al., 1998), suggesting that the basal release was partly mediated by reversal of Glu transport. However, it is worth to note that the spontaneous

release of [^{3}H]D-Asp was still higher (about 90%; p=0.026, $F_{(1,61)}$=16.964) in SOD1^{G93A} mice even in the presence of DL-TBOA.

Also the KCl-evoked (15 mM, 90 s pulse) overflow of [^{3}H]D-Asp was significantly more elevated (about 75%; p=0.027, $F_{(1,23)}$= 3.463) in SOD1^{G93A} mice at the pre-symptomatic stage of disease (Figure 1C). The overflow of [^{3}H]D-Asp was abolished in Ca^{2+}-free medium, both in SOD1 and SOD1^{G93A} mice, supporting the exocytotic origin of release, which includes also the surplus observed in SOD1^{G93A} mice. The 15 mM KCl-evoked release of [^{3}H]D-Asp was studied also in the presence of BoNt-C1 that cleaves SNAP 25 thus reducing synaptic vesicle docking and fusion (Foran et al., 1996). Figure 1C also shows that the depolarization-evoked [^{3}H]D-Asp overflow was significantly reduced (about 50% and 70% vs. SOD1 and SOD1^{G93A} mice respectively; p<0.001 and p<0.001; $F_{(1,16)}$= 181.769) in the presence of BoNt-C1, thus confirming the exocytotic origin of release. Noteworthy, BoNt-C1 abolished the excessive release of [^{3}H]D-Asp induced by KCl in SOD1^{G93A} mice. The toxin also obliterated the excessive [^{3}H]D-Asp basal release in SOD1^{G93A} mice (SOD1:3.78±0.32%; SOD1^{G93A}:5.51±0.24%; p<0.001; F(1,16)=8.355. SOD1/BoNt-C1: 4.05±0.16%; SOD1^{G93A}/BoNt-C1: 3.88±0.32%; p=0.662 $F_{(1,16)}$=8.355).

To further support the idea that the increase of [^{3}H]D-Asp overflow observed in SOD1^{G93A} mice was due to augmented exocytosis, we also studied the release of [^{3}H]D-Asp evoked by ionomycin, that induces neurotransmitter exocytotic release promoting Ca^{2+} influx into nerve terminals with no involvement of voltage-sensitive Ca^{2+} channels (VSCCs; Sanchez-Prieto et al. 1987). As shown in Figure 1D, ionomycin (0.3 μM, 90s pulse) stimulated the release of [^{3}H]D-Asp in spinal cord of SOD1 and SOD1^{G93A} mice. As observed with KCl, the amount of [^{3}H]D-Asp released by ionomycin was more pronounced (about 65%; p=0.017, $F_{(1,15)}$= 2.310) in SOD1^{G93A} mice than in controls. The effects of ionomycin were abrogated in the absence of Ca^2, also occluding the potentiation of [^{3}H]D-Asp release observed in SOD1^{G93A} mice in standard medium.

The experiments above show that the basal and the stimulus-evoked release of Glu are abnormal in the spinal cord of SOD1^{G93A} mice and that the augmented Glu release was exocytotic in nature.

Figure 1

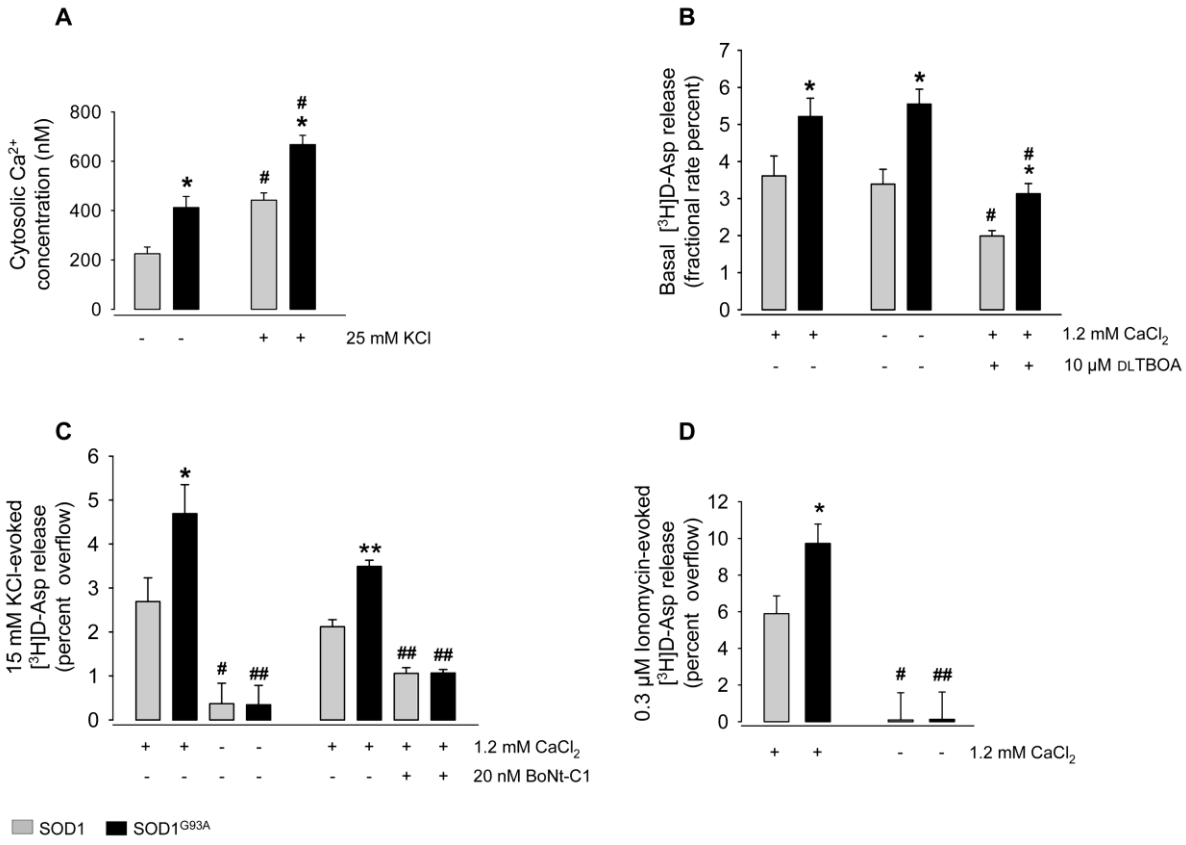

Figure 1. Cytosolic calcium and [^{3}H]D-Aspartate release in the spinal cord of pre-symptomatic SOD1^{G93A} mice. **(A)** $[Ca^{2+}]_c$ under resting and depolarizing (25 mM KCl) conditions in synaptosomes from the spinal cord of SOD1 and SOD1^{G93A} mice. Results are expressed as mean (nM) ± SEM of n=8-9 independent measurements. $^{*}p<0.001$ vs. the $[Ca^{2+}]_c$ in SOD1 mice; $^{\#}p<0.001$ vs. the respective basal $[Ca^{2+}]_c$ (two way ANOVA plus Bonferroni post hoc test). **(B)** Ca^{2+}- and DL-TBOA-dependency of the basal efflux of [^{3}H]D-Asp from spinal cord synaptosomes of SOD1 and SOD1^{G93A} mice. Results are expressed as fractional rate x 100 ± SEM of n=8-13 independent experiments run in triplicate. $^{*}p<0.05$ vs. the basal efflux in SOD1 mice; $^{\#}p<0.05$ vs. the respective basal outflow in standard medium (two way ANOVA plus Bonferroni post hoc test). **(C)** Ca^{2+}- and BoNT C1-dependency of the 15 mM KCl-evoked overflow of [3H]D-Asp from spinal cord synaptosomes of SOD1 and SOD1^{G93A} mice. Results are expressed as percent overflow ± SEM of n=4-9 independent experiments run in triplicate. $^{*}p<0.05$ and $^{**}p<0.001$ vs. the overflow in SOD1 mice; $^{\#}p<0.01$ and $^{\#\#}p < 0.001$ vs. the respective overflow in standard medium (two way ANOVA plus Bonferroni post hoc test). **(D)** Ca^{2+}-dependency of the ionomycin-evoked overflow of [^{3}H]D-Asp from spinal cord synaptosomes of SOD1 and SOD1^{G93A} mice. Results are expressed as percent overflow ± SEM of n=3-7 independent experiments run in triplicate. $^{*}p < 0.05$ vs. the overflow in SOD1 mice; $^{\#}p < 0.01$ and $^{\#\#}p < 0.001$ vs. the respective overflow (two way ANOVA plus Bonferroni post hoc test).

The release of [^{3}H]D-Asp induced by ionomycin or sucrose and after repeated KCl stimulation in SOD1^{G93A} mice

To gain functional information about the synaptic pool of vesicles involved in the augmented exocytosis of Glu in pre-symptomatic SOD1^{G93A} mice, we compared the release of [^{3}H]D-Asp induced by 15 or 25 mM KCl, 0.3 or 1 μM ionomycin or 150 mM sucrose. As shown in Figure 2A, the [^{3}H]D-Asp overflows evoked by 15 and 25 mM KCl were increased (about 84% and 55%, $p<0.001$ and $p=0.006$, respectively; $F_{(1,30)}=20.833$) in SOD1^{G93A} mice vs. the respective controls. At variance, increasing the ionomycin concentration from 0.3 to 1 μM produced a huge increase of the stimulus-evoked [^{3}H]D-Asp release and led to the disappearance of the abnormal overflow present in SOD1^{G93A} mice using 0.3 μM ionomycin. Figure 2A also shows that hypertonic sucrose (150 mM), which is known to provoke exocytosis mobilizing selectively the RRP of vesicles by an atypical Ca^{2+}-independent mechanism (Rosenmund and Stevens 1996), induced a substantial release of [^{3}H]D-Asp, comparable to that observed with 25 mM KCl or 0.3 μM ionomycin, which was, as expected, not reduced by omission of Ca^{2+} (not shown). Most interestingly, also the sucrose-induced [^{3}H]D-Asp overflow was significantly greater (about 45%; $p=0.008$, $t_{(15)}=-3.081$) in SOD1^{G93A} than in SOD1 mice.

The stimulus-induced [^{3}H]D-Asp overflow was also measured during application of two 15 or 25 mM KCl consecutive stimuli of 90 s (Bianchi et al., 2009; Milanese et al., 2011). Figure 2B shows that the stimulus-induced [^{3}H]D-Asp overflow remained constant during the first and second stimulation in SOD1 mice. On the contrary, a significant decrease (about 41%, $p=0.048$, $F_{(1,30)}=0.874$ in 15 mM KCl stimulus; about 52%, $p<0.001$, $F_{(1,25)}=5.738$ in 25 mM KCl stimulus) was observed during the second stimulation in SOD1^{G93A} mice.

These results support the hypothesis that the augmented [^{3}H]D-Asp release measured in the spinal cord of SOD1^{G93A} mice is driven by an augmented size of the RRP of vesicles

Figure 2

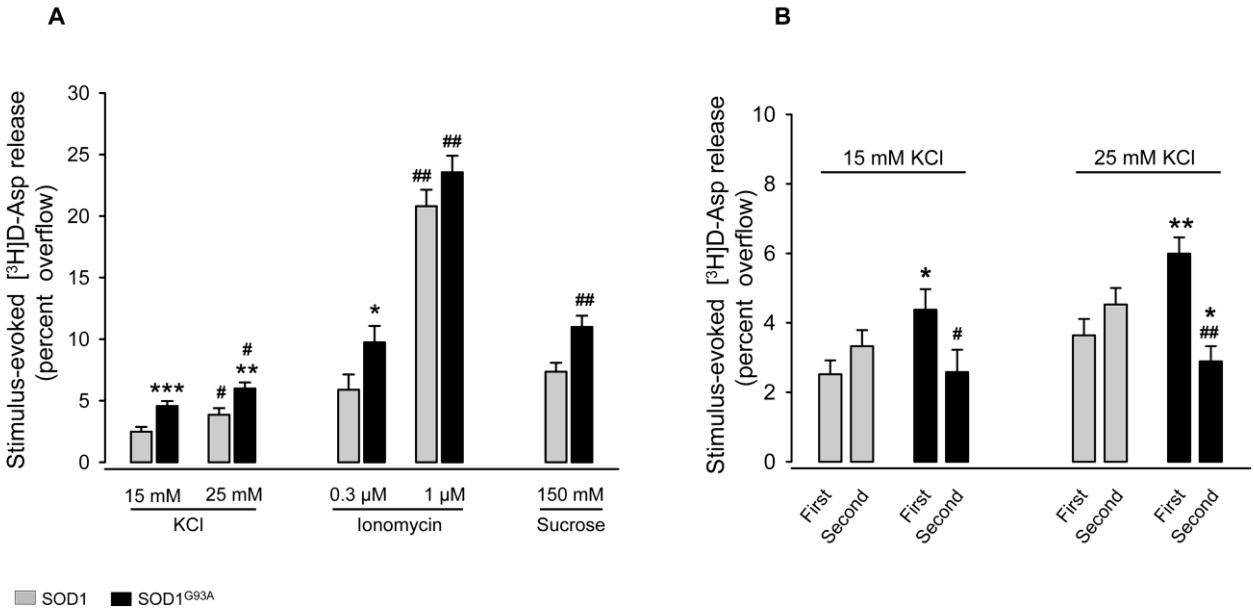

Figure 2. Single and repetitive stimulus-evoked overflow of [^{3}H]D-Aspartate in the spinal cord of pre-symptomatic SOD1^{G93A} mice. (A) KCl-, ionomycin- or sucrose-evoked overflow of [3H]D-Asp from spinal cord synaptosomes of SOD1 and SOD1^{G93A} mice. Results are expressed as percent overflow ± SEM of n=6-11 independent experiments run in triplicate. $^{*}p < 0.05$ $^{**}p < 0.01$ and $^{***}p < 0.001$ vs. the overflow in SOD1 mice; $^{\#}p < 0.05$ and $^{\#\#}p < 0.001$ vs. the respective 15mM KCl- and 0.3µM ionomycin-evoked overflow (two way ANOVA plus Bonferroni post hoc test and unpaired two-tailed Student's t-test). **(B)** KCl-evoked overflow of [^{3}H]D-Asp from spinal cord synaptosomes of SOD1 and SOD1^{G93A} mice after repetitive stimuli. Results are expressed as percent overflow ± SEM of n = 5-13 independent experiments run in triplicate. $^{*}p < 0.05$ and $^{**}p < 0.01$ vs. the overflow in SOD1 mice; $^{\#}p < 0.05$ and $^{\#\#}p < 0.001$ vs. the respective overflow (two way ANOVA plus Bonferroni post hoc test).

SNARE protein complexes are increased in pre-symptomatic SOD1^{G93A} mice

In order to shed light on the mechanisms supporting the augmented exocytotic release of [^{3}H]D-Asp in SOD1^{G93A} mice, we measured the amount of the three SNARE proteins, Stx-1, SNAP-25 and VAMP-2, and their assembly into SNARE complexes, mediating docking of synaptic vesicles (SVs) with presynaptic membranes at the active zone (Rizo and Xu, 2015), in SOD1 and SOD1^{G93A} mice. Neither Stx-1 nor VAMP-2 or SNAP-25 expression was modified in SOD1^{G93A} vs. SOD1 mice in synaptosomal membranes (Figure 3).

Figure 3

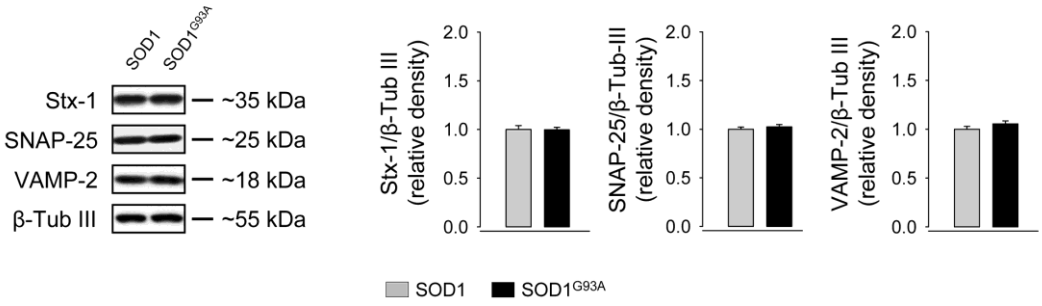

Figure 3. Expression of SNARE proteins in the spinal cord of pre-symptomatic SOD1 and SOD1^{G93A} mice. VAMP-2, Stx-1 and SNAP-25 were determined in synaptic membranes of SOD1 and SOD1^{G93A} mouse spinal cord. Cropped representative immunoreactive bands and quantitative analysis are reported. Immunoreactive bands are normalized for β-Tub III. Quantification is expressed as relative densities and represent the mean ± SEM of n=9 independent experiments. No significative differences were detected (unpaired two-tailed Student's t-test).

The association of the three SNARE proteins into SNARE complexes was evaluated in the non-denatured sinaptosomal membranes by immunoblotting the electrophoresed proteins using antibodies anti-Stx-1 and anti-VAMP-2. When challenged with the anti-Stx-1 antibody, four different SNARE complex bands were detected, with an apparent molecular weight of ~75, ~100, ~150, or ~200 kDa. As shown in Figure 4A the ~75 kDa complex was unchanged; instead, the higher molecular weight complexes were significantly augmented (about 50%, 65% and 70% in ~100, ~150, or ~200 kDa complexes, respectively; $p<0.001$, $t_{(6)}=-7.864$; $p=0.003$, $t_{(6)}=-4.795$ and $p=0.003$, $t_{(6)}=-4.885$). Considering that complexes consisting of only Stx-1 and SNAP-25 serve as intermediates in the SNARE complex assembly (Nicholson, et al., 1998), we also quantitated the accumulation of SNARE complexes containing VAMP-2. Also the levels of 100, 150 and 200 kDa VAMP-2-containing SNARE complexes were significantly increased (about 141%, 70% and 92%, in ~100, ~150, or ~200 kDa complexes, respectively; $p<0.001$, $t_{(6)}=-17.888$; $p<0.001$, $t_{(6)}=-12.523$ and $p<0.001$, $t_{(6)}=-7.549$) in synaptic membranes of SOD1^{G93A} mice (figure 4B), strongly suggesting an increase of active SNARE complexes at presynaptic membranes.

Since SNARE complexes mediate membrane fusion, these results suggest that the accumulation of presynaptic SNARE complexes in SOD1^{G93A} mice may be related to the abnormal Glu release measured in the spinal cord of these animals.

Figure 4

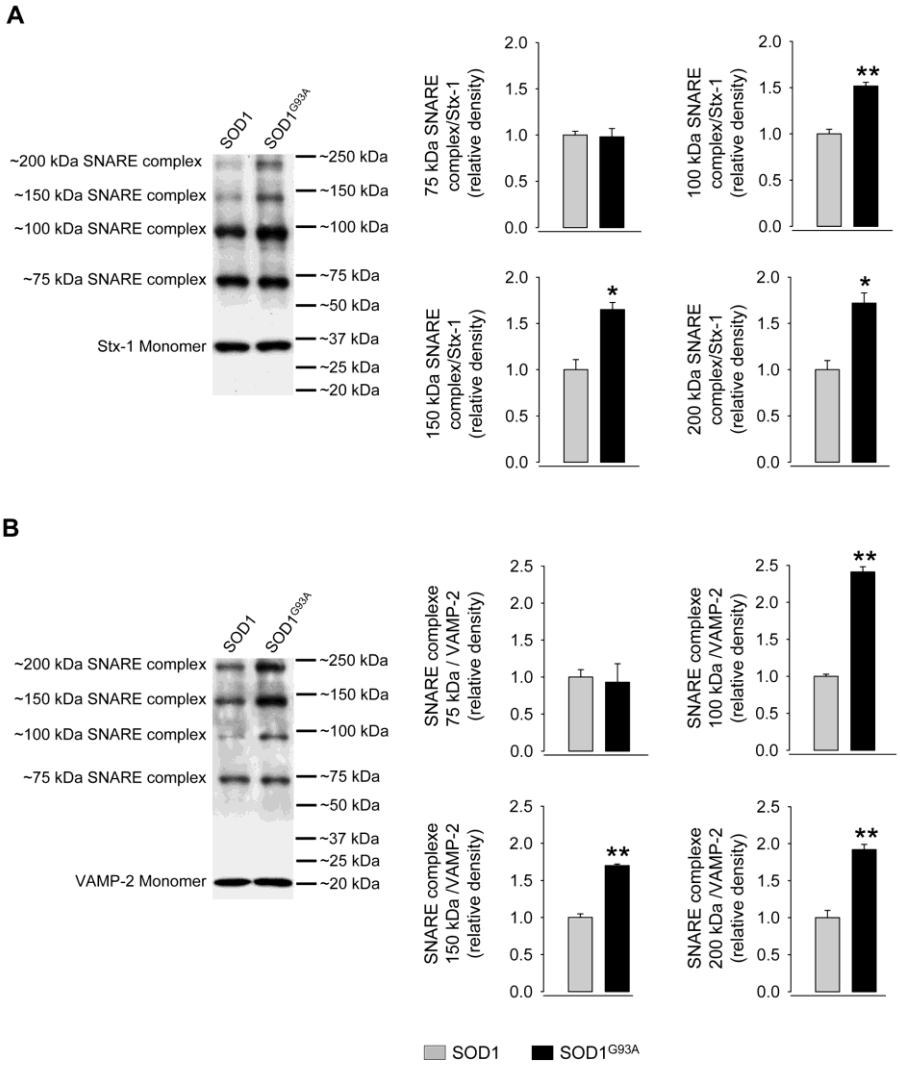

Figure 4. Expression of SNARE complexes in the spinal cord of pre-symptomatic SOD1^{G93A}. 75, 100, 150, and 200 kD SNARE complexes were determined in non-denaturated synaptosomal membranes of SOD1 and SOD1^{G93A} mice spinal cord, after immune-precipitation with antibodies against Stx-1 **(A)** or VAMP-2 **(B)**. Representative immunoreactive bands and quantitative analysis are reported. Immunoreactive bands are normalized for β-Tub-III. Quantification is expressed as relative densities and represent the mean ± SEM of n=4 independent experiments. $^{*}p < 0.01$ and $^{**}p < 0.001$ vs. SOD1 mice (unpaired two-tailed Student's t-test).

Expression of the presynaptic proteins synaptotagmin and actin is selectively augmented in pre-symptomatic SOD1^{G93A} mice

To get more insight into the changes of presynaptic mechanisms in SOD1^{G93A} mice, the expression of a number of proteins involved in the regulation of the SNARE complex formation or controlling docking, priming, fusion, and recycling of SVs was evaluated in synaptic membranes of synaptosomes prepared from the spinal cord of SOD1^{G93A} and SOD1 mice. We measured the expression of Syph-1, a protein that binds VAMP-2 and inhibits its interaction with the other SNARE proteins; Munc-18, a modulator of the conformation of Stx-1, that regulate the availability of this SNARE protein to assemble into complexes (Calakos and Scheller, 1994; Hata et al., 1993); Munc-13 and Rab-3a, proteins of the active zone that promote docking and priming of vesicles (Betz et al, 1997; Geppert et al., 1994); Syt-1, a vesicle protein acting as Ca^{2+} sensor for exocytosis, and its interacting protein Complexin-1/2 (Kelly, 1995; Roggero et al., 2007); NSF and the adapter proteins α/β-SNAP, involved in the dissociation of SNARE complexes, leading to vesicle priming and fusion (Woodman, 1997); Dynamin I, involved in the process of recycling of SVs (McClure and Robinson, 1996); β-Actin and Myosin Va, two cytoskeletal proteins involved in the trafficking of SVs within the nerve terminal (Doussau and Augustine, 2000; Rudolf et el., 2011).

Figure 5 shows that the expression of all the presynaptic proteins studied did not differ between the two mouse strains, with the exception of Syt-1 and β-Actin, which were significantly increased (about 15% and 30%, respectively; $p=0.045$, $t_{(16)}=-2.178$ and $p<0.001$, $t_{(16)}=-6.228$).

These results indicate that Syt-1, a key presynaptic calcium sensor, and β-Actin, a key cytoskeletal protein, are modified in the spinal cord of SOD1^{G93A} mice. The expression changes of these two proteins may be causally related to the changes of Glu release.

Figure 5

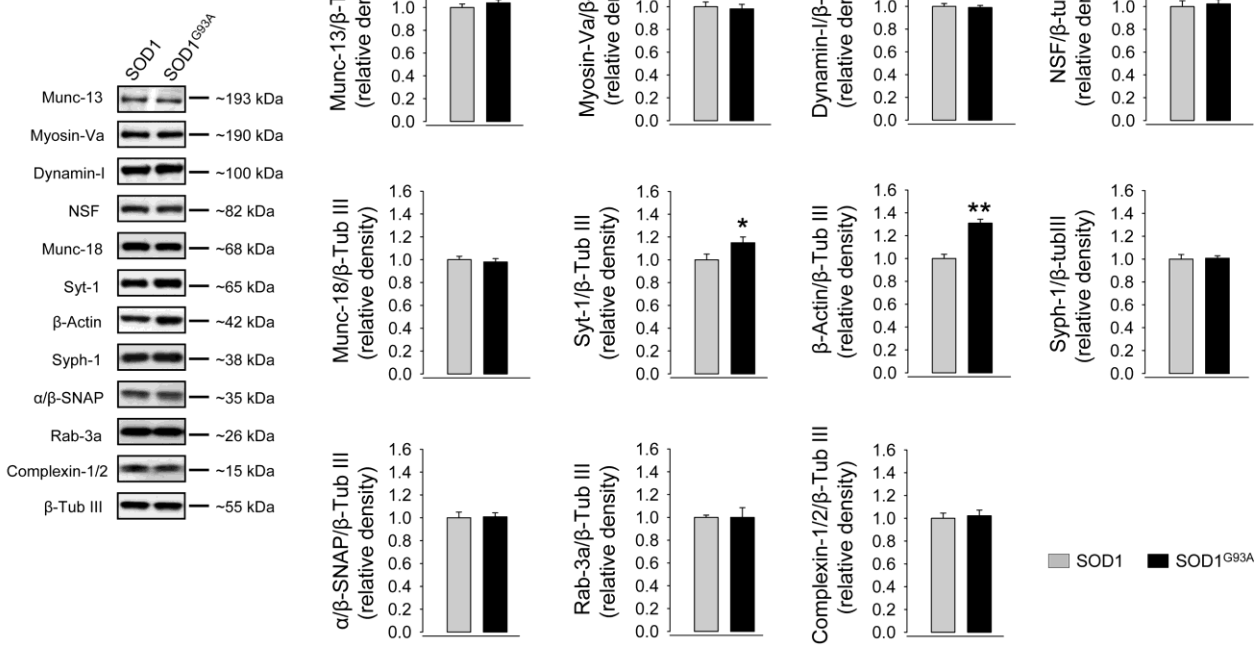

Figure 5. Expression of synaptic proteins in the spinal cord of pre-symptomatic SOD1^{G93A} mice. Syph-1, Munc-18, Munc-13, Rab-3a, Syt-1, Complexin-1/2, NSF, α/β-SNAP, Dynamin-I, β-Actin and Myosin-Va were determined in synaptosomal membranes of SOD1 and SOD1^{G93A} mice. Cropped representative immunoreactive bands and quantitative analysis are reported. Immunoreactive bands are normalized for β-Tub III. Quantification is expressed as relative densities and represent the mean ± SEM of n=8,9 independent experiments. $^{*}p < 0.05$ vs. SOD1 mice (unpaired two-tailed Student's t-test).

GSK-3 phosphorylation and activation are altered in pre-symptomatic SOD1^{G93A} mice

Previous studies showed that GSK-3, when activated, inhibits exocytosis by interacting with SNARE proteins (Zhu et al., 2007). We measured the expression level of the α and β isoforms of GSK-3 in presynaptic membranes of synaptosomes prepared from the spinal cord of SOD1 and SOD1^{G93A} mice and found a significantly increased expression of both GSK-3α and of GSK-3β isoforms (about 35% and 20% respectively; $p=0.001$, $t_{(16)}=-3.891$ and $p=0.002$, $t_{(16)}=-3.639$) in SOD1^{G93A} mice (Figure 6), thus suggesting an increase of its activity, since the enzyme is constitutively operative (Woodgett et al., 1993). However, the analysis of the phosphorylation state of GSK-3 in SOD1^{G93A} mice, by means of site-specific phospho-specific antibodies, revealed increased phosphorylation at Ser^{21} GSK-3α and at Ser^{9} GSK-3β (about 45% and 20% respectively; $p=0.001$, $t_{(16)}=-3.958$ and $p=0.006$, $t_{(16)}=-3.127$), an occurrence that reduces the activity of both the isoforms. As shown in Figure 6, no significant changes where observed in the phosphorylation at Tyr^{279} GSK-3α or at Tyr^{216} GSK-3β, which both promote the enzyme activity (Jope and Johnson, 2004).

These results suggest that, although GSK-3 expression is higher, inhibition of its activity by phosphorylation may play a role in the abnormal exocytosis observed in SOD1^{G93A} mice, by favouring the SNARE complex assembly.

Figure 6

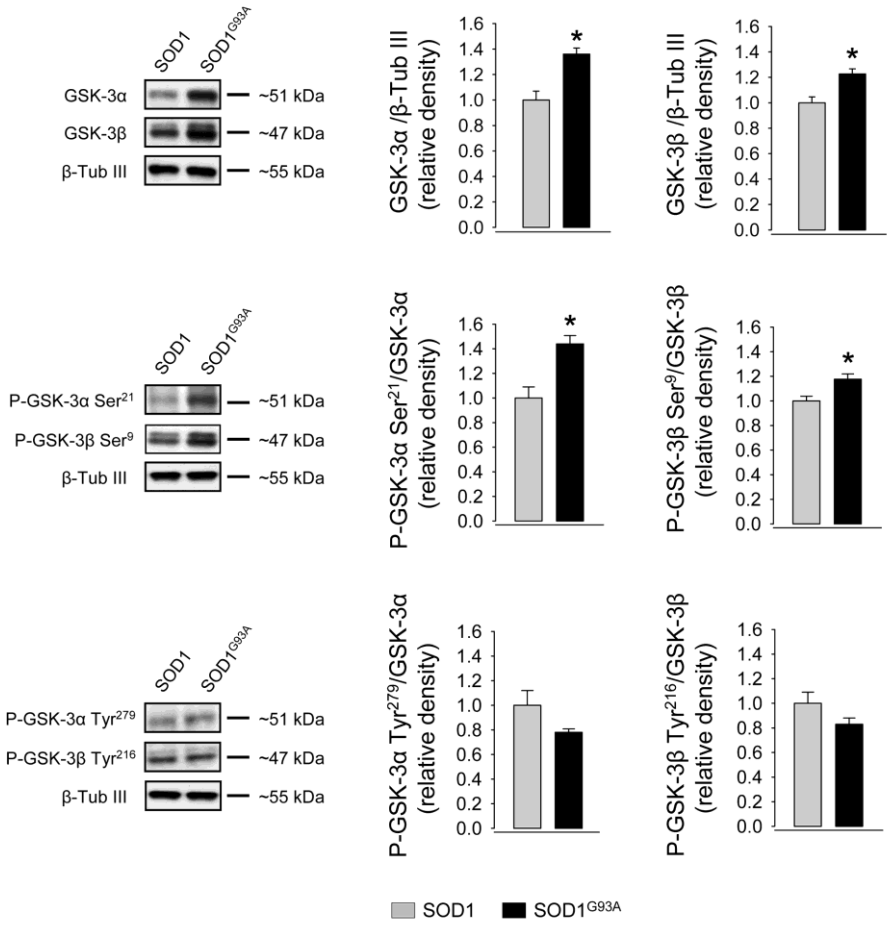

Figure 6. Expression and phosphorylation state of GSK-3 in the spinal cord of pre-symptomatic SOD1 and SOD1^{G93A} mice. GSK-3α and GSK-3β **(A)**, phosphorylated GSK-3α **(B)** and phosphorylated GSK-3β **(C)** were determined in synaptosomal membranes of pre-symptomatic SOD1 and SOD1^{G93A} mice. Cropped representative immunoreactive bands and quantitative analysis are reported. Immunoreactive bands of total GSK-3α or total GSK-3β are normalized for β-Tub III; immunoreactive bands of phorphor-GSK-3α or phorphor-GSK-3β were normalized for total GSK-3α and total GSK-3β, respectively. Quantification is expressed as relative densities and represent the mean ± SEM of n=9 independent experiments. $^{*}p < 0.01$ and $^{**}p < 0.001$ vs. SOD1 mice (unpaired two-tailed Student's t-test).

Synapsin-I phosphorylation state is increased in pre-symptomatic SOD1^{G93A} mice

Syn-I expression in the spinal cord of SOD1^{G93A} mice was not modified when compared to SOD1 mice (Figure 7A). The phosphate incorporation was separately analysed at site 1, which is phosphorylated by protein kinase A and calcium calmodulin-dependent kinase-I/IV (Czernik et al., 1987; Kasahara et al, 2000), at sites 3, which is phosphorylated by CaMK-II (Huttner and Greengard, 1979; Sihra et al., 1989), and at sites 4/5, which are phosphorylated by ERK-1 and -2 (Chi et al, 2003; Jovanovic et al., 1996), by using phosphorylation state-specific antibodies. Interestingly, all sites displayed increased phosphorylation levels (about 75%, 85% and 35% as to sites 1, 3, and 4/5, respectively; $p=0.017$, $t_{(10)}=-2.857$, $p=0.029$, $t_{(10)}=-2.554$ and $p=0.036$, $t_{(10)}=-2.427$) in SOD1^{G93A} mice (Figure 7A).

To clarify whether the more pronounced phosphorylation of Syn-I could be causally linked to the excessive Glu release found in spinal cord of pre-symptomatic SOD1^{G93A} mice, we performed release experiments exposing synaptosomes purified from SOD1 and SOD1^{G93A} mice to 15 mM KCl after entrapping antibodies able to selectively bind the epitope including the phosphorylation site 1 (Ser^9; Ab1) or the proline-rich D-domain (Ab2) of Syn-I. As shown in Figure 7B, the release of [^{3}H]D-Asp induced by 15 mM KCl in SOD1 mice was not modified by Ab1, but was strongly reduced (about 67% $p=0.012$, $F_{(1,32)}=26.255$) by Ab2. Most important, both antibodies abolished the 15 mM KCl-evoked potentiation of neurotransmitter release present in SOD1^{G93A} mice (about 57% and 80% in Ab1 and Ab2 condition, respectively; $p<0.001$, $F_{(1,32)}=26.255$).

Interestingly, Ab1 and Ab2 reduced also the excessive release of [^{3}H]D-Asp detected in SOD1^{G93A} mice under basal conditions, (SOD1 2.81±0.33%; SOD1^{G93A} 4.27±0.33%; $p=0.004$; SOD1/Ab1 3.88±0.36%; SOD1^{G93A}/Ab1: 3.33±0.36%; $p=0.289$; SOD1/Ab2: 3.21±0.36%; SOD1^{G93A}/Ab2: 4.09±0.36%; $p=0.09$; $F_{(1,32)}=4.419$), further supporting the idea that the surplus of [^{3}H]D-Asp release under resting conditions is driven by fusion of primed vesicle that are augmented at the nerve terminal membrane.

These results suggest that the augmented exocytosis can be maintained by an increased size of the RRP of vesicles that are mobilized from the cytoskeleton due to the increased Syn-I phosphorylation state.

Figure 7

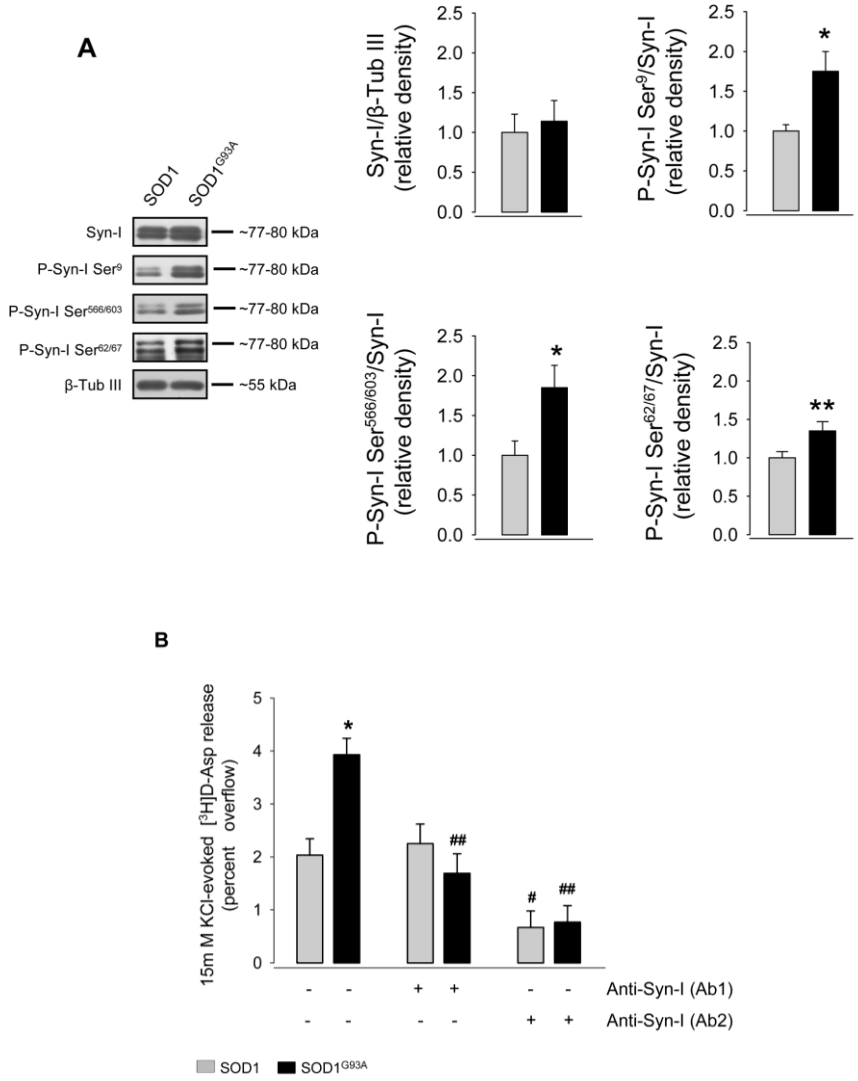

Figure 7. Expression and phosphorylation state of synapsin I and significance for [^{3}H]D-Aspartate release in the spinal cord of pre-symptomatic SOD1^{G93A} mice. (A) Syn-I and its phosphorylation state at sites 1, 3 and 4/5 were determined in synaptosomal lysates of SOD1 and SOD1^{G93A} mice. Cropped representative immunoreactive bands and quantitative analysis are reported. Immunoreactive bands of total Syn-I were normalized for β-Tub III; immunoreactive bands of phospho-Syn-I were normalized for total Syn-I. Quantification is expressed as relative densities and represent the mean ± SEM of n=6 independent experiments. $^{*}p < 0.05$ and $^{**}p < 0.01$ vs. SOD1 mice (unpaired two-tailed Student's t-test). **(B)** The overflow of [3H]D-Asp evoked by 15 mM KCl was measured in synaptosomes of SOD1 and SOD1^{G93A} mice entrapped with antibodies anti-Syn-I at site 1 (Ser^9; Ab1) or proline rich D-domains (Ab2) during their preparation. Results are expressed as percent overflow ± SEM of n = 5,7 independent experiments run in triplicate. *p < 0.001 vs. the overflow in SOD1 mice; $^{\#}p < 0.05$ and $^{\#\#}p < 0.001$ vs. the respective overflow (two way ANOVA plus Bonferroni post hoc test).

Discussion

The basal and the stimulus-evoked exocytotic release of Glu are enhanced in the spinal cord of 30 days-old pre-symptomatic SOD1^{G93A} mice. Our results also revealed: **(*i*)** rise of the nerve terminal $[Ca^{2+}]_c$; **(*ii*)** augmentation of assembled SNARE complexes; **(*iii*)** increased Syt-1 and β-Actin expression; **(*iv*)** augmented phosphorylation of GSK-3 inhibitory sites; **(*v*)** augmented phosphorylation of Syn-I **(*vi*)** increased RRP of vesicles, **(*vii*)** facilitation of Glu release.

Basal release and stimulus-evoked overflow of Glu are enhanced in SOD1^{G93A} mice.

The basal release of Glu is augmented in pre-symptomatic SOD1^{G93A} mice and this over-release could be detected also in presence of DL-TBOA, excluding that it takes place through reversal of Glu transporters and suggesting that it is exocytotic, likely due to Ca^{2+}-independent random vesicle fusion, sustained by the increase of the RRP of vesicles and the number of SNARE complexes (see below). This hypothesis is reinforced by the disappearance of the abnormal release in SOD1^{G93A} mouse synaptosomes pre-treated with BoNt-C1 or entrapped with anti-synapsin-I antibodies. The KCl-evoked Glu overflow in SOD1^{G93A} and SOD1 mice was abolished by omission of Ca^{2+}, suggesting that both overflows and its surplus in SOD1^{G93A} mice are due to exocytosis. A number of observations support the exocytotic origin of the excessive Glu overflow: ionomycin, which promotes exocytosis inducing Ca^{2+} influx into nerve terminals independently from VSCCs (Sanchez-Prieto et al., 1987; Verhage et al., 1991), also produced excessive Glu overflow in SOD1^{G93A} mice that was abolished in the absence of Ca^{2+}; hypertonic sucrose, which induces Ca^{2+}-independent exocytosis selectively involving the RRP of vesicles (Lonart and Sudhof, 2000; Rosenmund and Stevens, 1996), provoked Glu release that was abnormally increased in SOD1^{G93A} mice; hydrolysis of SNAP-25 by BoNt-C1 or inhibition of Syn-I activity abolished the surplus of release in SOD1^{G93A} mice.

Altered signalling mechanisms may account for the enhanced Glu release in SOD1^{G93A} mice.

Homeostasis of Ca^{2+} is altered in pre-symptomatic SOD1^{G93A} mouse spinal cord synaptosomes, leading to increased $[Ca^{2+}]_c$. Intracellular Ca^{2+} has been previously found increased in MN nerve terminals of biopsied human ALS muscles and in animal models of familial ALS with SOD1 mutations, also at early stages of disease (Siklos et al., 1999). Likely, Ca^{2+} plays a role in the excessive Glu exocytosis, either by directly affecting fusion of vesicles or by modulating processes leading to release facilitation. In this framework, we previously proved the Ca^{2+}-induced hyper-activation of CaMK-II in late symptomatic SOD1^{G93A} mice and the resulting phosphorylation of Syn-I at site 3 (Milanese et al., 2011).

The phosphorylation state of GSK is altered in SOD1^{G93A} mice. This kinase interacts with proteins regulating exocytosis, by promoting or inhibiting the SNARE complex formation (Zhu et al., 2010; 2007). Phosphorylation of Tyr^{279} GSK-3α or Tyr^{216} GSK-3β enhances its enzymatic activity, while phosphorylation of Ser^{21} GSK-3α or Ser^{9} GSK-3β significantly decreases active site availability (Lochhead et al, 2001). The elevated phosphorylation of the inhibitory sites, with no changes at the activatory sites, suggests that the GSK-driven inhibition of SNARE complex formation is hampered in SOD1^{G93A} mice and may account for the elevated number of assembled SNARE complexes. Also Syn-I phosphorylation is increased in pre-symptomatic SOD1^{G93A} mice, leading to mobilization of SVs from the reserve pool to the RRP, a mechanism that increases the availability of vesicles for release (Benfenati et al., 1989; Ceccaldi et al., 1995; Chi et al., 2003; Hvalby et al., 2006).

Selective changes in presynaptic proteins may support the enhanced Glu release in SOD1^{G93A} mice.

Presynaptic proteins of the release machinery regulate exocytosis by modulating the size of the SV pools and vesicle trafficking between these pools, as well as SNARE complex assembly/disassembly. Among the proteins analyzed, only Syt-1 and β-Actin expressions were significantly increased. Increase of Syt-1 is of particular interest also in view of the higher $[Ca^{2+}]_c$.

The concomitant elevated expression of the Ca^{2+} sensor protein and the higher Ca^{2+} availability might account for a more elevated probability of primed vesicles to fuse. β-Actin represents a major component of the cellular scaffold and plays important roles in shaping excitatory synapse activity (Matus et al., 1982). It has been suggested that β-Actin dynamism would facilitate exocytosis, while β-Actin filament stabilization would have the opposite effect (Cingolani and Goda, 2008). However, the barrier function of β-Actin has been recently challenged since the numbers of docked/primed vesicles and their fusion rate were higher in hippocampal synapses of mice lacking β-Actin depolymerizing factor and cofilin-1, where synaptic β-Actin cytoskeleton is less dynamic (Wolf et al., 2015). Further, we have reported that the proteolytic activity of calpain is enhanced in $SOD1^{G93A}$ mice at early and late disease stages (Stifanese et al, 2014; 2010). Excessively activated calpain cleaves synaptic proteins, which regulate β-Actin polymerization state (Chimura et al., 2015), possibly affecting exocytosis. Due to these apparently conflicting evidences, further studies are needed to clarify the role of β-Actin dysregulation in $SOD1^{G93A}$ mice.

Increased RRP of vesicles is a main factor for the enhancement of Glu release in $SOD1^{G93A}$ mice.

Our evidence strongly suggests that the abnormal exocytotic Glu release is mainly based on augmented size of the RRP of vesicles at spinal glutamatergic synapses of $SOD1^{G93A}$ mice and on increased release facilitation, sustained by enhanced $[Ca^{2+}]_c$ and/or expression of Syt-1. Direct measurements of release validated the assumption that altered synaptic efficiency in $SOD1^{G93A}$ mice is mainly based on augmentation of the RRP of glutamatergic vesicles. The excessive Glu release was abolished by entrapping antibodies binding either the phosphorylation site 1 of Syn-I, independently of its phospho/de-phospho state, or the proline rich D-domains in the synaptosomal cytoplasm, thus indicating that the activity of Syn-I is causally linked to the alteration of exocytosis. Additionally, the ionomycin-induced abnormal Glu release disappeared when ionomycin concentration was raised, recruiting SV pools other than the RRP (Ashton and Dolly, 2000; Stigliani et al., 2003), thus obscuring the RRP contribution to release. Finally, the overflow of

[^{3}H]D-Asp induced by hypertonic sucrose, known to trigger SV exocytosis exclusively from the RRP, was higher in SOD1^{G93A} mice.

An attracting aspect of the present results is that both the basal release and the stimulus-evoked overflow of Glu were more pronounced in SOD1^{G93A} mice as early as at 30 days of life, before the appearance of the first signs of motor neuron degeneration and clinical symptoms (Bendotti et al., 2001; Oliván et al., 2015), thus supporting the idea that these modifications are related to the mutation itself and not to the worsening of MN conditions during disease progression and that, therefore, they represent a causative factor rather than an effect of the pathology. When comparing the present results to those in late symptomatic SOD1^{G93A} mice (Milanese et al., 2011), it seems that the excessive Glu release is largely based on a similar mechanistic ground, indicating that excessive exocytosis is due to precocious alterations of presynaptic mechanisms that remain effective along the mouse life.

The abnormal basal release suggests the continuous presence of an excessive amount of Glu in the synapse, thus sustaining pre- and post-synaptic receptor activation. We have recently reported that release-promoting presynaptic Group I mGluRs of SOD1^{G93A} mice are activated *in-vitro* by nanomolar concentrations of the mGluR1 and mGluR5 agonist (S)-3,5-Dihydroxyphenylglycine (Giribaldi et al., 2013) and that knocking-down mGluR1 in SOD1^{G93A} mice has a very favourable impact on survival and clinical progression (Milanese et al., 2014). The increased affinity of agonists for Group I mGluRs and the excessive basal release of Glu may account for a tonic activation of mGluRs in SOD1^{G93A} mice that accompanies the phasic over-activation of pre- and post-synaptic Glu receptor due to the abnormal stimulus-evoked Glu overflow.

We have also shown that excessive Glu release in SOD1^{G93A} mice can take place also following activation of glycine and GABA transporters, heterologously sited on Glu-releasing nerve terminals (heterotransporters; Bonanno et al., 1993; Raiteri et al., 2005, 2004, 2003).

Although heterotransporter-induced and exocytosis-driven excessive Glu release have been long perceived as different phenomena, they present a number of similarities and a recent paper attempted to reconcile the two events in a unique view, suggesting that the heterotransporter-induced abnormal Glu release represents an epiphenomenon of the augmented exocytosis (Milanese et al., 2015).

Targeting Glu release in ALS may have remarkable advantages. ALS is a multifactorial disease and the lack of effective biomarkers to distinguish patients according to the aetiology recommends that a successful therapy should also be multimodal. Thus, targeting an early up-stream phenomenon such as abnormal Glu release may affect different down-stream pathways at the postsynaptic level, mimicking a multimodal therapy. The evidence that riluzole, which acts by reducing the release of Glu, only slightly prolongs survival in ALS patients (Cheung et al., 2006; Louvel et al., 1997), may weaken the hypothesis. However, it should be recalled that riluzole is mainly a Na^+ channel blocker (Urbani and Belluzzi, 2000; Zona et al., 1998) that non-specifically inhibits the release of neurotransmitters, both excitatory and inhibitory. A more direct approach to the inhibition of Glu release/transmission should guarantee a better success.

Conclusions

The exocytotic release of Glu is abnormal in the $SOD1^{G93A}$ mouse model of ALS and this phenomenon is detectable as early as at post-natal day 30, leading to the conclusion that the disregulation of Glu release may represent a pivotal feature for pathology onset and development. Discrete presynaptic molecular modifications, eventually leading to the increase of the RRP of vesicles, are at the basis of the changes observed and are largely maintained during the disease progress and worsening. Altered presynaptic mechanisms leading to the augmentation of the RRP

of vesicle and to enhanced exocytosis may represent targets for novel pharmacological approaches to reduce excitotoxicity in ALS.

Acknowledgements:

This work was supported by research grants from the Italian Ministry of University (PRIN projects n. 2006058401, to GB, and n. 2006058401, to F.O. and SIR project n. RBSI14B1Z1, to M.M.) . We thank Dr. Paul Greengard (The Rockefeller University, New York City, NY) for generously providing the antibody to phospho-Ser$^{566/603}$ (site 3) of Synapsin-I.

The authors gratefully acknowledge Drs. Giulia Treccani and Elisabetta Calloni for technical help.

The authors declare no competing financial interests.

Bibliography

Andersen, P.M., Al-Chalabi, A., 2011. Clinical genetics of amyotrophic lateral sclerosis: what do we really know? Nat. Rev. Neurol. 7, 603-615.

Ashton, A.C., Dolly, J.O., 2000. A late phase of exocytosis from synaptosomes induced by elevated $[Ca2+]_i$ is not blocked by Clostridial neurotoxins. J. Neurochem. 74, 1979-1988.

Bendotti, C., Calvaresi, N., Chiveri, L., Prelle, A., Moggio, M., Braga, M., Silani, V., De Biasi, S., 2001. Early vacuolization and mitochondrial damage in motor neurons of FALS mice are not associated with apoptosis or with changes in cytochrome oxidase histochemical reactivity. J. Neurol. Sci. 191, 25-33.

Benfenati, F., Valtorta, F., Bähler, M., Greengard, P. 1989., Synapsin I, a neuron-specific phosphoprotein interacting with small synaptic vesicles and F-Actin. Cell. Biol. Int. Rep. 13, 1007-1021.

Betz, A., Okamoto, M., Benseler, F., Brose, N., 1997. Direct interaction of the rat unc-13 homologue Munc13–1 with the N terminus of syntaxin. J. Biol. Chem. 272, 2520–2526.

Bianchi, V., Farisello, P., Baldelli, P., Meskenaite, V., Milanese, M., Vecellio, M., Mühlemann, S., Lipp, H.P., Bonanno, G., Benfenati, F., Toniolo, D., D'Adamo, P., 2009. Cognitive impairment in Gdi1-deficient mice is associated with altered synaptic vesicle pools and short-term synaptic plasticity, and can be corrected by appropriate learning training. Hum. Mol. Genet. 18, 105-117.

Birve, A., Neuwirth, C., Weber, M., Marklund, S.L., Nilsson, A.C., Jonsson. P.A., Andersen, P.M., 2010. A novel SOD1 splice site mutation associated with familial ALS revealed by SOD activity analysis. Hum. Mol. Genet. 19, 4201-4206.

Boillée, S., Yamanaka, K., Lobsiger, C.S., Copeland, N.G., Jenkins, N.A., Kassiotis, G., Kollias, G., Cleveland, D.W., 2006. Onset and progression in inherited ALS determined by motor neurons and microglia. Science 312, 1389-1392.

Bonanno, G., Pittaluga, A., Fedele, E., Fontana, G., Raiteri, M., 1993. Glutamic acid and gamma-aminobutyric acid modulate each other's release through heterocarriers sited on the axon terminals of rat brain. J. Neurochem. 61, 222-230.

Bonanno, G., Giambelli, R., Raiteri, L., Tiraboschi, E., Zappettini, S., Musazzi, L., Raiteri, M., Racagni, G., Popoli, M., 2005. Chronic antidepressants reduce depolarization-evoked glutamate release and protein interactions favoring formation of SNARE complex in hippocampus. J. Neurosci. 25, 3270-3279.

Bradford, M.M., 1976. A rapid and sensitive method for the quantitation of microgram quantities of protein utilizing the principle of protein-dye binding. Anal. Biochem. 72, 248-254.

Brown, R.H. Jr., 1995. Amyotrophic lateral sclerosis: recent insights from genetics and transgenic mice. Cell 80, 687-692.

Calakos, N., Scheller, R.H., 1994. Vesicle-associated membrane protein and synaptophysin are associated on the synaptic vesicle. J. Biol. Chem. 269, 24534-24537.

Ceccaldi, P.E, Grohovaz, F., Benfenati, F., Chieregatti, E., Greengard, P., Valtorta, F., 1995. Dephosphorylated synapsin I anchors synaptic vesicles to actin cytoskeleton: an analysis by videomicroscopy. J. Cell. Biol. 128, 905-912.

Cheung, Y.K., Gordon, P.H., Levin, B., 2006. Selecting promising ALS therapies in clinical trials. Neurology 67, 1748-1751.

Chi, P., Greengard, P., Ryan, T.A., 2003. Synaptic vesicle mobilization is regulated by distinct synapsin I phosphorylation pathways at different frequencies. Neuron 38, 69-78.

Chi, P., Greengard, P., Ryan, T.A., 2001. Synapsin dispersion and reclustering during synaptic activity. Nat. Neurosci, 4, 1187-1193.

Chimura, T., Launey, T., Yoshida, N., 2015. Calpain-mediated degradation of drebrin by excitotoxicity in vitro and in vivo. PLoS One 10, e0125119.

Cingolani, L.A., Goda, Y., 2008. Actin in action: the interplay between the actin cytoskeleton and synaptic efficacy. Nat. Rev. Neurosci. 9, 344-356.

Cleveland, D.W., Rothstein, J.D., 2001. From Charcot to Lou Gehrig: deciphering selective motor neuron death in ALS. Nat. Rev. Neurosci. 2, 806-19.

Cleveland, D.W., Bruijn, L.I., Wong, P.C., Marszalek, J.R., Vechio, J.D., Lee, M.K., Xu, X.S., Borchelt, D.R., Sisodia, S.S., Price, D.L., 1996. Mechanisms of selective motor neuron death in transgenic mouse models of motor neuron disease. Neurology 47, 54–62.

Corona, J.C., Tapia, R., 2004. AMPA receptor activation, but not the accumulation of endogenous extracellular glutamate, induces paralysis and motor neuron death in rat spinal cord in vivo. J. Neurochem. 89, 988–997.

Czernik, A.J., Pang, D.T., Greengard, P., 1987. Amino acid sequences surrounding the cAMP-dependent and calcium/calmodulin-dependent phosphorylation sites in rat and bovine synapsin I. Proc. Natl. Acad. Sci. U S A 84, 7518-7522.

Doussau, F., Augustine, G.J., 2000. The actin cytoskeleton and neurotransmitter release: an overview. Biochimie 82, 353-363.

Eisen, A., 2009. Amyotrophic lateral sclerosis: A 40-year personal perspective. J. Clin. Neurosci. 16, 505-512.

Fleck, M.W., Barrionuevo, G., Palmer, A.M., 2001. Synaptosomal and vesicular accumulation of L-glutamate, L- aspartate and D- aspartate. Neurochem. Int. 39, 217–225.

Foran, P., Lawrence, G.W., Shone, C.C., Foster, K.A., Dolly, J.O., 1996. Botulinum neurotoxin C1 cleaves both syntaxin and SNAP-25 in intact and permeabilized chromaffin cells: correlation with its blockade of catecholamine release. Biochemistry 35, 2630-2636.

Geppert, M., Bolshakov, V.Y., Siegelbaum, S.A., Takei, K., De Camilli, P., Hammer, R.E., Südhof TC., 1994. The role of Rab3A in neurotransmitter release. Nature 369, 493-497.

Giribaldi, F., Milanese, M., Bonifacino, T., Rossi, P.I.A., Di Prisco, S., Pittaluga, A., Tacchetti, C., Puliti, A., Usai, C., Bonanno, G., 2013. Group I metabotropic glutamate autoreceptors induce abnormal glutamate exocytosis in a mouse model of amyotrophic lateral sclerosis. Neuropharmacology 66, 253-263.

Goll, D.E., Thompson, V.F., Li, H., Wei, W., Cong, J., 2003. The calpain system. Physiol. Rev. 83, 731-801.

Grynkiewicz, G., Poenie, M., Tsien, R.Y., 1985. A new generation of Ca2+ indicators with greatly improved fluorescence properties. J. Biol. Chem. 260, 3440-3450.

Gurney, M.E., Pu, H., Chiu, A.Y., Dal Canto, M.C., Polchow, C.Y., Alexander, D.D., Caliendo, J., Hentati, A., Kwon, Y.W., Deng, H.X., et al., 1994. Motor neuron degeneration in mice that express a human Cu,Zn superoxide dismutase mutation. Science 264, 1772-1775. Erratum in: Science 269(5221), 149.

Haidet-Phillips, A.M., Hester, M.E., Miranda, C.J., Meyer, K., Braun, L., Frakes, A., Song, S., Likhite, S., Murtha, M.J., Foust, K.D., Rao, M., Eagle, A., Kammesheidt, A., Christensen, A., Mendell, J.R., Burghes, A.H., Kaspar, B.K., 2011. Astrocytes from familial and sporadic ALS patients are toxic to motor neurons. Nat. Biotechnol. 29, 824-828.

Hata, Y., Slaughter, C.A., Südhof, T.C., 1993. Synaptic vesicle fusion complex contains unc-18 homologue bound to syntaxin. Nature 366, 347-351.

Hu, J.H., Zhang, H., Wagey, R., Krieger, C., Pelech, S.L., 2003. Protein kinase and protein phosphatase expression in amyotrophic lateral sclerosis spinal cord. J. Neurochem. 85, 432-442.

Huttner, W.B., Greengard, P., 1979. Multiple phosphorylation sites in protein I and their differential regulation by cyclic AMP and calcium. Proc. Natl. Acad. Sci. U S A 76, 5402-5406.

Hvalby, Ø., Jensen, V., Kao, H.T., Walaas, S.I., 2006. Synapsin-regulated synaptic transmission from readily releasable synaptic vesicles in excitatory hippocampal synapses in mice. J. Physiol. 571, 75-82.

Ilieva, H., Polymenidou, M., Cleveland, D.W., 2009. Non-cell autonomous toxicity in neurodegenerative disorders: ALS and beyond. J. Cell. Biol. 187, 761-772.

Jope, R.S., Johnson, G.V., 2004. The glamour and gloom of glycogen synthase kinase-3. Trends Biochem. Sci. 29, 95-102.

Jovanovic, J.N., Benfenati, F., Siow, Y.L., Sihra, T.S., Sanghera, J.S., Pelech, S.L, Greengard, P., Czernik, A.J., 1996. Neurotrophins stimulate phosphorylation of synapsin I by MAP kinase and regulate synapsin I-actin interactions. Proc. Natl. Acad. Sci. USA 93, 3679–3683.

Kasahara, J., Fukunaga, K., Miyamoto, E., 2000. Activation of CA(2+)/calmodulin-dependent protein kinase IV in cultured rat hippocampal neurons. J. Neurosci. Res. 59, 594-600.

Kelly, R.B., 1995. Neural transmission. Synaptotagmin is just a calcium sensor. Curr. Biol. 5, 257-259.

King, A.E., Woodhouse, A., Kirkcaldie, M.T.K., Vickers, J.C., 2016. Excitotoxicity in ALS: Overstimulation, or overreaction? Experimental Neurology 275, 162–171.

Kuner, R., Groom, A.J., Müller, G., Kornau, H.C., Stefovska, V., Bresink, I., Hartmann, B., Tschauner, K., Waibel, S., Ludolph, A.C., Ikonomidou, C., Seeburg, P.H., Turski, L., 2005.

Mechanisms of disease: motoneuron disease aggravated by transgenic expression of a functionally modified AMPA receptor subunit. Ann. N Y Acad. Sci. 1053, 269-286.

Laemmli, U.K., 1970. Cleavage of structural proteins during the assembly of the head of bacteriophage T4. Nature 227, 680–685.

Lochhead, P.A., Coghlan, M., Rice, S.Q., Sutherland, C., 2001. Inhibition of GSK-3 selectively reduces glucose-6-phosphatase and phosphatase and phosphoenolypyruvate carboxykinase gene expression. Diabetes 50, 937-946.

Lonart, G., Südhof, T.C., 2000. Assembly of SNARE core complexes prior to neurotransmitter release sets the readily releasable pool of synaptic vesicles. J. Biol. Chem. 275, 27703-27707.

Louvel, E., Hugon, J., Doble, A., 1997. Therapeutic advances in amyotrophic lateral sclerosis. Trends Pharmacol. Sci. 18, 196-203.

Matus, A., Ackermann, M., Pehling, G., Byers, H.R., Fujiwara, K., 1982. High actin concentrations in brain dendritic spines and postsynaptic densities. Proc. Natl. Acad. Sci. U S A 79, 7590-7594.

McClure, S.J., Robinson, P.J., 1996. Dynamin, endocytosis and intracellular signaling. Mol. Membr. Biol. 13, 189-215.

Milanese, M., Bonifacino, T., Fedele, E., Rebosio, C., Cattaneo, L., Benfenati, F., Usai, C., Bonanno, G., 2015. Exocytosis regulates trafficking of GABA and glycine heterotransporters in spinal cord glutamatergic synapses: a mechanism for the excessive heterotransporter-induced release of glutamate in experimental amyotrophic lateral sclerosis. Neurobiol. Dis. 74, 314-324.

Milanese, M., Giribaldi, F., Melone, M., Bonifacino, T., Musante, I., Carminati, E., Rossi, P.I., Vergani, L., Voci, A., Conti, F., Puliti, A., Bonanno, G., 2014. Knocking down metabotropic

glutamate receptor 1 improves survival and disease progression in the SOD1(G93A) mouse model of amyotrophic lateral sclerosis. Neurobiol. Dis. 64, 48-59.

Milanese, M., Zappettini, S., Onofri, F., Musazzi, L., Tardito, D., Bonifacino, T., Messa, M., Racagni, G., Usai, C., Benfenati, F., Popoli, M., Bonanno, G., 2011. Abnormal exocytotic release of glutamate in a mouse model of amyotrophic lateral sclerosis. J. Neurochem. 116, 1028-1042.

Morrison, B.M., and Morrison, J.H., 1999. Amyotrophic lateral sclerosis associated with mutations in superoxide dismutase: a putative mechanism of degeneration. Brain Res. Rev. 29, 121–135.

Mulder, D.W., Kurland, L.T., Offord, K.P., Beard, C.M., 1986. Familial adult motor neuron disease: Amyotrophic lateral sclerosis. Neurology 36, 511-517.

Musazzi, L., Rimland, J.M., Ieraci, A., Racagni, G., Domenici, E., Popoli, M., 2014. Pharmacological characterization of BDNF promoters I, II and IV reveals that serotonin and norepinephrine input is sufficient for transcription activation. Int. J. Neuropsychopharmacol. 17, 779-791.

Musazzi, L., Milanese, M., Farisello, P., Zappettini, S., Tardito, D., Barbiero, V.S., Bonifacino, T., Mallei, A., Baldelli, P., Racagni, G., Raiteri, M., Benfenati, F., Bonanno, G., Popoli, M., 2010. Acute stress increases depolarization-evoked glutamate release in the rat prefrontal/frontal cortex: the dampening action of antidepressants. PLoS One 5(1), e8566.

Nicholson, K.L., Munson, M., Miller, R.B., Filip, T.J., Fairman, R., Hughson, F.M., 1998. Regulation of SNARE complex assembly by an N-terminal domain of the t-SNARE Sso1p. Nat. Struct. Biol. 5, 793-802.

Oliván, S., Calvo, A.C., Rando, A., Muñoz, M.J., Zaragoza, P., Osta, R., 2015. Comparative study of behavioural tests in the SOD1G93A mouse model of amyotrophic lateral sclerosis. Exp. Anim. 64, 147-153.

Perry, T.L., Krieger, C., Hansen, S., Eisen, A., 1990. Amyotrophic lateral sclerosis: amino acid levels in plasma and cerebrospinal fluid. Ann. Neurol. 28, 12-17.

Peters, O.M., Ghasemi, M., Brown, R.H.Jr., 2015. Emerging mechanisms of molecular pathology in ALS. J. Clin. Invest. 125, 2548.

Raiteri, L., Stigliani, S., Usai, C., Diaspro, A., Paluzzi, S., Milanese, M., Raiteri, M., Bonanno, G., 2008. Functional expression of release-regulating glycine transporters GLYT1 on GABAergic neurons and GLYT2 on astrocytes in mouse spinal cord. Neurochem. Int. 52, 103-112.

Raiteri, L., Zappettini, S., Milanese, M., Fedele, E., Raiteri, M., Bonanno, G., 2007. Mechanisms of glutamate release elicited in rat cerebrocortical nerve endings by 'pathologically' elevated extraterminal K+ concentrations. J. Neurochem. 103, 952–961.

Raiteri, L., Zappettini, S., Stigliani, S., Paluzzi, S., Raiteri, M., Bonanno, G., 2005. Glutamate release induced by activation of glycine and GABA transporters in spinal cord is enhanced in a mouse model of amyotrophic lateral sclerosis. Neurotoxicology 26, 883-892.

Raiteri, L., Stigliani, S., Zappettini, S., Mercuri, N.B., Raiteri, M., Bonanno, G., 2004. Excessive and precocious glutamate release in a mouse model of amyotrophic lateral sclerosis. Neuropharmacology 46, 782-792.

Raiteri, L., Paolucci, E., Prisco, S., Raiteri, M., Bonanno, G., 2003. Activation of a glycine transporter on spinal cord neurons causes enhanced glutamate release in a mouse model of amyotrophic lateral sclerosis. Br. J. Pharmacol. 138, 1021-1025.

Raiteri, L., Raiteri, M., Bonanno, G., 2002. Coexistence and function of different neurotransmitter transporters in the plasma membrane of CNS neurons. Prog. Neurobiol. 68, 287-309.

Raiteri, M., Sala, R., Fassio, A., Rossetto, O., Bonanno, G., 2000. Entrapping of impermeant probes of different size into nonpermeabilized synaptosomes as a method to study presynaptic mechanisms. J. Neurochem. 74, 423-31.

Raiteri, M., Bonanno, G., Marchi, M., Maura, G., 1984. Is there a functional linkage between neurotransmitter uptake mechanisms and presynaptic receptors? J. Pharmacol. Exp. Ther. 231, 671-677.

Rizo, J., Xu, J., 2015. The Synaptic Vesicle Release Machinery. Annu. Rev. Biophys. 44, 339-367.

Roggero, C.M., De Blas, G.A., Dai, H., Tomes, C.N., Rizo, J., Mayorga, L.S., 2007. Complexin/synaptotagmin interplay controls acrosomal exocytosis. J. Biol. Chem. 282, 26335-26343.

Rosen, D.R., 1993. Mutations in Cu/Zn superoxide dismutase gene are associated with familial amyotrophic lateral sclerosis. Nature 364, 362.

Rosenmund, C., Stevens, C.F., 1996. Definition of the readily releasable pool of vesicles at hippocampal synapses. Neuron 16, 1197-1207.

Rothstein, J.D., Van Kammen, M., Levey, A.I., Martin, L.J., Kuncl, R.W., 1995. Selective loss of glial glutamate transporter GLT-1 in amyotrophic lateral sclerosis. Ann. Neurol. 38, 73-84.

Rothstein, J.D., Tsai, G., Kuncl, R.W., Clawson, L., Cornblath, D.R., Drachman, D.B., Pestronk, A., Stauch, B.L., Coyle, J.T., 1990. Abnormal excitatory amino acid metabolism in amyotrophic lateral sclerosis. Ann. Neurol. 28, 18-25.

Rudolf, R., Bittins, C.M., Gerdes, H.H., 2011. The role of myosin V in exocytosis and synaptic plasticity. J. Neurochem. 116,177-191.

Sanchez-Prieto, J., Sihra, T.S., Nicholls, D.G., 1987. Characterization of the exocytotic release of glutamate from guinea-pig cerebral cortical synaptosomes. J. Neurochem. 49, 58-64.

Shaw, P.J., Eggett, C.J., 2000. Molecular factors underlying selective vulnerability of motor neurons to neurodegeneration in amyotrophic lateral sclerosis. J. Neurol. 247 Suppl 1, I17-27.

Shaw, P.J., Forrest, V., Ince, P.G., Richardson, J.P., Wastell, H.J., 1995. CSF and plasma amino acid levels in motor neuron disease: elevation of CSF glutamate in a subset of patients. Neurodegeneration 4, 209–216.

Shimamoto, K., Lebrun, B., Yasuda-Kamatani, Y., Sakaitani, M., Shigeri, Y., Yumoto, N., Nakajima, T., 1998. DL-threo-beta-benzyloxyaspartate, a potent blocker of excitatory amino acid transporters. Mol. Pharmacol. 53, 195-201.

Sihra, T.S., Wang, J.K., Gorelick, F.S., Greengard, P., 1989. Translocation of synapsin I in response to depolarization of isolated nerve terminals. Proc. Natl. Acad. Sci. U S A 86, 8108-8112.

Siklós, L., Engelhardt, J.I., Adalbert, R., Appel, S.H., 1999. Calcium-containing endosomes at oculomotor terminals in animal models of ALS. Neuroreport 10, 2539-2545.

Spreux-Varoquaux, O., Bensimon, G., Lacomblez, L., Salachas, F., Pradat, P.F., Le Forestier, N., Marouan, A., Dib, M., Meininger, V., 2002. Glutamate levels in cerebrospinal fluid in amyotrophic lateral sclerosis: a reappraisal using a new HPLC method with coulometric detection in a large cohort of patients. J. Neurol. Sci. 193, 73–78.

Stifanese, R., Averna, M., De Tullio, R., Pedrazzi, M., Milanese, M., Bonifacino, T., Bonanno, G., Salamino, F., Pontremoli, S., Melloni, E., 2014. Role of calpain-1 in the early phase of experimental ALS. Arch. Biochem. Biophys. 562, 1-8.

Stifanese, R., Averna, M., De Tullio, R., Pedrazzi, M., Beccaria, F., Salamino, F., Milanese, M., Bonanno, G., Pontremoli, S., Melloni, E., 2010. Adaptive modifications in the

calpain/calpastatin system in brain cells after persistent alteration in Ca2+ homeostasis. J. Biol. Chem. 285, 631-643.

Stigliani, S., Raiteri, L., Fassio, A., Bonanno, G., 2003. The sensitivity of catecholamine release to botulinum toxin C1 and E suggests selective targeting of vesicles set into the readily releasable pool. J. Neurochem. 85, 409-421.

Tan, W., Pasinelli, P., Trotti, D., 2014. Role of mitochondria in mutant SOD1 linked amyotrophic lateral sclerosis. Biochim. Biophys. Acta 1842, 1295-1301.

Tortarolo, M., Grignaschi, G., Calvaresi, N., Zennaro, E., Spaltro, G., Colovic, M., Fracasso, C., Guiso, G., Elger, B., Schneider, H., Seilheimer, B., Caccia, S., Bendotti, C., 2006. Glutamate AMPA receptors change in motor neurons of SOD1G93A transgenic mice and their inhibition by a concompetitive antagonist ameliorates the progression of amytrophic lateral sclerosis-like disease. J. Neurosci. Res. 83, 134-146.

Tovar-Y-Romo, L.B., Santa-Cruz, L.D., Zepeda, A., Tapia, R., 2009. Chronic elevation of extracellular glutamate due to transport blockade is innocuous for spinal motoneurons in vivo. Neurochem. Int. 54, 186–191.

Treccani, G., Musazzi, L., Perego, C., Milanese, M., Nava, N., Bonifacino, T., Lamanna, J., Malgaroli, A., Drago, F., Racagni, G., Nyengaard, J.R., Wegener, G., Bonanno, G., Popoli, M., 2014. Stress and corticosterone increase the readily releasable pool of glutamate vesicles in synaptic terminals of prefrontal and frontal cortex. Mol. Psychiatry 19, 433-443.

Urbani, A., Belluzzi, O., 2000. Riluzole inhibits the persistent sodium current in mammalian CNS neurons. Eur. J. Neurosci. 12, 3567-3574.

Van Damme, P., Dewil, M., Robberecht, W., Van Den Bosch, L., 2005. Excitotoxicity and amyotrophic lateral sclerosis. Neurodegener. Dis. 2, 147–159.

Van Den Bosch, L., Van Damme, P., Bogaert, E., Robberecht, W., 2006. The role of excitotoxicity in the pathogenesis of amyotrophic lateral sclerosis. Biochim. Biophys. Acta 1762, 1068-1082.

Van Den Bosch, L., Vandenberghe, W., Klaassen, H., Van Houtte, E., Robberecht, W., 2000. Ca(2+)-permeable AMPA receptors and selective vulnerability of motor neurons. J. Neurol. Sci. 180, 29-34.

Verhage, M., McMahon, H.T., Ghijsen, W.E., Boomsma, F., Scholten, G., Wiegant, V.M., Nicholls, D.G., 1991. Differential release of amino acids, neuropeptides, and catecholamines from isolated nerve terminals. Neuron 6, 517-524.

Wang, L., Nadler, J.V., 2007. Reduced aspartate release from rat hippocampal synaptosomes loaded with clostridial toxin light chain by electroporation: evidence for an exocytotic mechanism. Neurosci. Lett. 412, 239–242.

Wolf, M., Zimmermann, A.M., Görlich, A., Gurniak, C.B., Sassoè-Pognetto, M., Friauf, E., Witke, W., Rust, M.B., 2015. ADF/Cofilin Controls Synaptic Actin Dynamics and Regulates Synaptic Vesicle Mobilization and Exocytosis. Cereb. Cortex 25, 2863-2875.

Woodgett, J.R., Plyte, S.E., Pulverer, B.J., Mitchell, J.A., Hughes, K., 1993. Roles of glycogen synthase kinase-3 in signal transduction. Biochem. Soc. Trans. 21, 905-907.

Woodman, P.G., 1997. The roles of NSF, SNAPs and SNAREs during membrane fusion. Biochim. Biophys. Acta 1357, 155-172.

Wuolikainen, A., Moritz, T., Marklund, S.L., Antti, H., Andersen, P.M., 2011. Disease-related changes in the cerebrospinal fluid metabolome in amyotrophic lateral sclerosis detected by GC/TOFMS. PLoS One 6, e17947 17910.11371/journal.pone.0017947.

Zhu, L.Q., Liu, D., Hu, J., Cheng, J., Wang, S.H., Wang, Q., Wang, F., Chen, J.G., Wang, J.Z., 2010. GSK-3 beta inhibits presynaptic vesicle exocytosis by phosphorylating P/Q-type calcium channel and interrupting SNARE complex formation. J. Neurosci. 30, 3624-3633.

Zhu, L.Q., Wang, S.H., Liu, D., Yin, Y.Y., Tian, Q., Wang, X.C., Wang, Q., Chen, J.G., Wang, J.Z., 2007. Activation of glycogen synthase kinase-3 inhibits long-term potentiation with synapse-associated impairments. J. Neurosci. 27, 12211-12220.

Zona, C., Siniscalchi, A., Mercuri, N.B., Bernardi, G., 1998. Riluzole interacts with voltage-activated sodium and potassium currents in cultured rat cortical neurons. Neuroscience 85, 931-938